Emergent Vibronic Excitations in the Magnetodielectric Regime of Ce_2O_3

A. Sethi,[1,*] J. E. Slimak,[1] T. Kolodiazhnyi,[2] and S. L. Cooper[1,†]
[1]Department of Physics and Materials Research Laboratory, University of Illinois, Urbana, Illinois 61801, USA
[2]National Institute for Materials Science, 1-1 Namiki, Tsukuba, Ibaraki, 305-0044, Japan

(Received 11 January 2019; revised manuscript received 1 March 2019; published 29 April 2019)

The strong coupling between spin, lattice, and electronic degrees of freedom in magnetic materials can produce interesting phenomena, including multiferroic and magnetodielectric (MD) behavior, and exotic coupled excitations, such as electromagnons. We present a temperature- and magnetic field–dependent inelastic light (Raman) scattering study that reveals the emergence of vibronic modes, i.e., coupled vibrational and crystal-electric-field (CEF) electronic excitations, in the unconventional rare-earth MD material Ce_2O_3. The energies and intensities of these emergent vibronic modes are indicative of enhanced vibronic coupling and increased modulation of the dielectric susceptibility in the Néel state ($T_N \approx 6.2$ K). The field dependences of the energies and intensities of these vibronic modes are consistent with a decrease of both the vibronic coupling and the dielectric fluctuations associated with these modes below T_N. These results suggest a distinctive mechanism for MD behavior in Ce_2O_3 that is associated with a field-tunable coupling between CEF and phonon states.

DOI: 10.1103/PhysRevLett.122.177601

Introduction.—Magnetically responsive materials, including multiferroics [1] and magnetodielectrics [2], are of enormous scientific and technological interest because the physical properties of these materials have large susceptibilities to external perturbations, such as magnetic field and pressure. These large susceptibilities reflect a strong coupling between spin, electronic, and lattice degrees of freedom, one manifestation of which is the emergence of coupled excitations, such as hybrid magnon-phonon modes (i.e., electromagnons) in the magnetoelectric phase of multiferroic materials [1,3–9]. A key challenge remains elucidating the underlying spin-lattice coupling mechanisms governing magnetically responsive phases and their associated hybrid excitations [1].

Multiferroic and magnetodielectric materials most commonly involve transition metal (TM) compounds, in which the presence of magnetic frustration and the resultant complex magnetic orders are key factors responsible for their multiferroic properties [1–5,8,9]. The search for new magnetically responsive materials is important, not only to expand the family of existing multiferroics but also to uncover the novel physics that new materials may exhibit.

Recently, a giant magnetodielectric (MD) response was reported in the hexagonal A-type rare-earth oxide, Ce_2O_3 [10]. This material does not exhibit any complex magnetic ordering typical of TM compounds; consequently, the mechanism associated with MD behavior in Ce_2O_3 remains an open issue. Significantly, the localized f orbitals in rare-earth materials lead to CEF excitations within the f electron manifold that are energetically resonant with the phonon bands [11–17]. This condition can lead to strong vibronic coupling between the crystal-electric-field (CEF) and phonon excitations [12–17], offering the possibility of novel spin-lattice coupling mechanisms and magnetically responsive phenomena in rare earth–based materials.

In this Letter, we report Raman scattering studies showing that the MD phase below T_N in Ce_2O_3 is characterized by the emergence of hybrid "vibronic" excitations, involving coupled f-electron CEF and phonon modes. The energies and intensities of these vibronic modes are consistent with a rapid enhancement of the vibronic coupling and an increased modulation of the dielectric susceptibility by these coupled modes below T_N in Ce_2O_3. Magnetic field–dependent Raman measurements show that an applied field decreases both the vibronic coupling and the modulation of the dielectric susceptibility below T_N. These results suggest that the field-dependent coupling between the electronic and phononic degrees of freedom in the Néel state is associated with a distinctive mechanism for MD behavior in Ce_2O_3.

Experimental methods.—The polycrystalline Ce_2O_3 samples used for this study were prepared and characterized as per the methods described in Ref. [10]. Raman scattering measurements were performed using a 647.1 nm excitation line of a Kr^+ laser. To minimize laser heating of the samples, the laser was focused to a ~50 μm diameter spot and incident powers between 0.5 and 3 mW were used. The minimal effects of laser heating at these low laser powers were estimated using a procedure discussed in the Supplemental Material [18], and these quantitative estimates are accounted for in the temperatures reported in this Letter. The scattered light was collected in a backscattering geometry, dispersed through a triple stage spectrometer, and then recorded with a liquid nitrogen

cooled charge-coupled-device detector. Samples were inserted in a helium flow-through cryostat, which was horizontally mounted in the bore of a superconducting magnet to allow simultaneous temperature (3–300 K) and magnetic (0–9T) measurements. All magnetic measurements were performed in a Faraday geometry with the incident light wave vector parallel to the magnetic field ($\boldsymbol{k}\|\boldsymbol{H}$) and perpendicular to the surface of the sample.

Phonons for $T > T_N$.—*A*-type Ce_2O_3 belongs to the trigonal $P\bar{3}2/m1$ or D^3_{3d} space group [10,19–21]. Group theory predicts four Raman active phonons for this crystal structure, $2A_{1g} + 2E_g$ [19–21]. Figure 1 shows the temperature dependences of the expected phonons in the paramagnetic phase of Ce_2O_3. The measured phonon energies at $T = 295$ K are in close agreement with a previous room temperature Raman scattering study [19]. The two lower energy phonons shown in Figs. 1(a) and 1(b) at $\omega \approx 103.8$ and 188.5 cm^{-1} correspond to the bending vibrations of the Ce-O(II) bond with E_g and A_{1g} symmetry, respectively [19,20]. The increasing background of the phonon in Fig. 1(b) is caused by a nearby CEF excitation that will be discussed later. The broad peak in Fig. 1(c) at $\omega \approx 408$ cm^{-1} (at $T = 295$ K) is composed of two closely spaced A_{1g}- and E_g-symmetry phonons, which are associated with the stretching vibrations of the long and short Ce-O (II) bonds, respectively [19–21]. In unpolarized Raman scattering studies at room temperature, the stretching A_{1g} and E_g phonons were not energy resolved in previous studies of the rare-earth (RE) sesquioxides (RE_2O_3), including Ce_2O_3 [19,20]. However, at 9 K, we can clearly distinguish both the phonons at $\omega_{A_{1g}} \approx 408.6$ and $\omega_{E_g} \approx 416$ cm^{-1}.

Crystal-electric-field excitations for $T > T_N$.—In addition to the phonons, two broad peaks exhibiting strongly temperature-dependent energies and intensities are observed at low temperatures, as shown in Figs. 2(a) and 2(b). With increasing temperature, these modes decrease in intensity, which is consistent with the temperature dependences expected for CEF excitations. Indeed, the energies of these two peaks correspond well with the CEF excitations calculated for the lower-lying CEF transitions within crystal-field-split $J = 5/2$ manifold of states in Ce_2O_3 [10,11]. To our knowledge, the excitations at $\omega \approx 230$ and 805 cm^{-1} (at $T = 9$ K) shown in Fig. 2 are the first reported experimental observation of CEF excitations in Ce_2O_3.

Notably, the CEF excitation energies exhibit anomalous temperature dependences, initially decreasing with decreasing temperature from 295 to 50 K, but then increasing in energy with decreasing temperature below 50 K. This anomalous temperature dependence is suggestive of strong electron-phonon coupling involving the CEF excitations in Ce_2O_3.

Vibronic modes and phonon anomalies for $T < T_N$.—In the Néel state, two new modes develop [see Fig. 3(a)]: a sharp mode at $\omega_1 \approx 177$ cm^{-1} and a broader mode at $\omega_2 \approx 250$ cm^{-1}. Below T_N, the mode at ω_2 gains intensity while the 230 cm^{-1} CEF_1 excitation loses intensity, suggesting that there is a transfer of spectral weight from CEF_1 to the ω_2 mode with decreasing temperature through T_N.

We can rule out interpreting these new modes as magnons or electromagnons. First, the energies of the

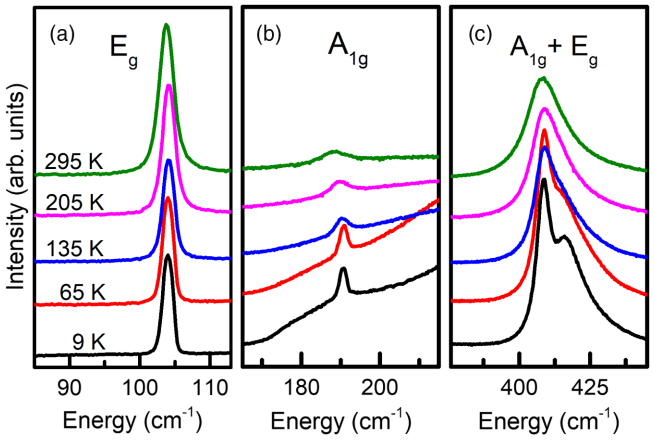

FIG. 1. Temperature dependences of Raman intensities of zone-center phonons for $T > T_N$.

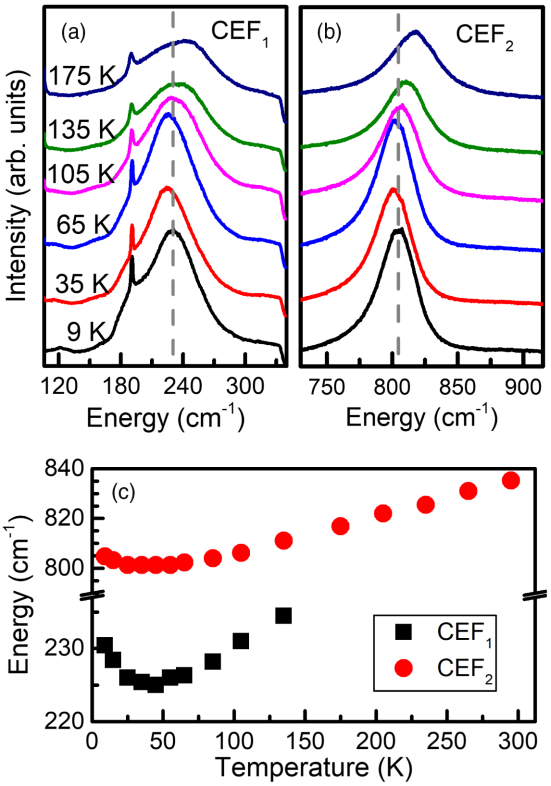

FIG. 2. (a), (b) Temperature dependences of Raman intensities of CEF excitations in Ce_2O_3 for $T > T_N$. The dashed lines are a guide to the eye showing the shifts in energies of the two peaks with temperature. (c) Summary of temperature dependences of CEF excitation energies.

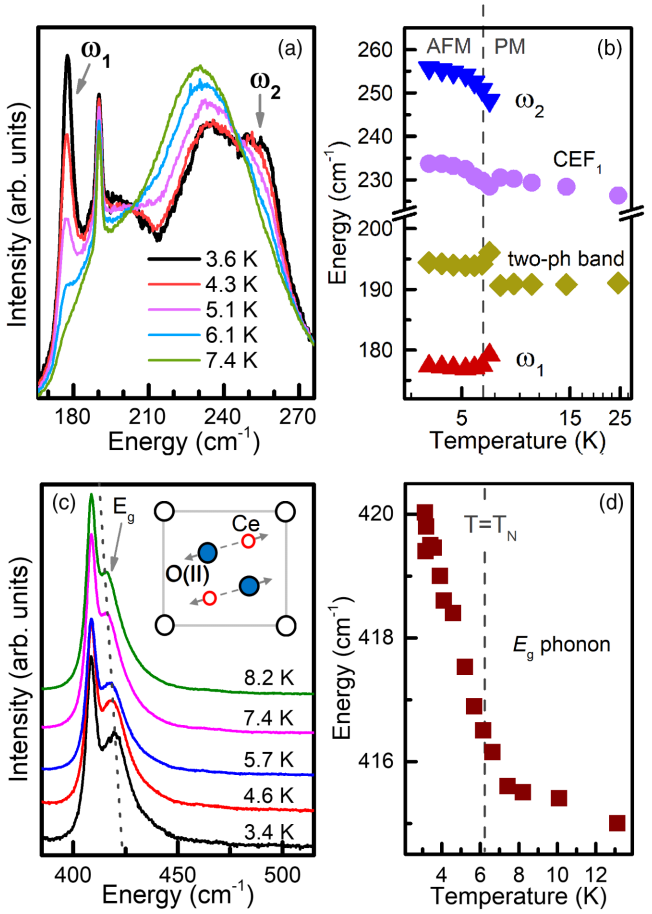

FIG. 3. (a) Raman spectrum of vibronic modes, ω_1 and ω_2, as a function of temperature. (b) Summary of (log scale) temperature dependences of energies of ω_1, ω_2, CEF_1, and two-ph band. Symbol size used is larger than the fitting errors in peak positions. (c) Temperature dependence of Raman spectrum of the stretching E_g phonon across T_N. Dotted line is a guide to the eye. Inset: schematic of E_g symmetry stretching vibration of Ce-O(II) bond, adapted from Refs. [19–21]. Small empty circles denote Ce ion, and large shaded circles denote O(II) ions. The large empty circles at the corners denote O(I) ions which do not participate in Raman active vibrations. Vertical axis is the c_3 axis. (d) Summary of dependence of E_g phonon energy on temperature across T_N. Dashed line in (b) and (d) denotes $T = T_N$ boundary between the antiferromagnetic (AFM) and paramagnetic (PM) phases.

modes at ω_1 and ω_2 are roughly an order of magnitude too large for zone-center magnons or electromagnons given the low magnetic ordering temperature ($T_N \approx 6.2$ K) of Ce_2O_3. In particular, other Ce-based compounds with comparable Néel temperatures have magnon energies in the range 8–35 cm^{-1} [22–26], well below the energies of the two new modes observed in Ce_2O_3. Second, the energies and lifetimes of modes at ω_1 and ω_2 do not show the temperature dependences expected for magnetic excitations. Lastly, linear magnetoelectric materials such as Ce_2O_3 require an external magnetic field to excite electromagnons [10], whereas we observe both new modes even in the absence of an applied field.

On the other hand, the two emergent modes in the magnetodielectric Néel state of Ce_2O_3 have all the characteristics of vibronic excitations, i.e., coupled vibrational and f-electron quantum modes. Thalmeier and Fulde first predicted that strong electron-phonon coupling between a crystal field level and an energetically proximate phonon band can lead to two "vibronic" states having mixed electron-phonon character [12]; such vibronic modes have been observed in many rare-earth compounds with atomiclike crystal field levels in the phonon energy region, including $CeAl_2$ [12], $CeCu_2$ [13], $Ho_2Ti_2O_7$ [14], $CeCuAl_3$ [15], and $NdBa_2Cu_3O_7$ [16]. Several characteristics identify the two new modes observed below T_N in Ce_2O_3 as vibronic modes involving the CEF_1 level and a phonon band: first, the development of two new modes, ω_1 and ω_2, in the same energy region as the CEF_1 and phonon modes is consistent with the vibronic mode interpretation, as shown more quantitatively below. Second, the increasing separation between the ω_1 and ω_2 mode energies with decreasing temperature [see Figs. 3(a) and 3(b)] is consistent with an increasing level repulsion associated with increasing vibronic coupling within the Thalmeier-Fulde vibronic model. Finally, the transfer of scattering strength from the electronic CEF_1 excitation to the broader vibronic mode is strong evidence for mixed electronic character associated with the ω_2 mode.

In addition to the emergent vibronic modes, a broad feature at $\omega \approx 194$ cm^{-1} develops at low temperatures, especially below 7 K (for clarity, see Fig. S1 in the Supplemental Material [18]). Because the four expected single-phonon excitations and the two CEF excitations in this energy range have already been accounted for, this broad feature likely involves a two-phonon band that is involved in the formation of the vibronic modes. Figure 3(b) summarizes the temperature dependences of the peak energies of the two vibronic modes, the CEF_1 excitation, and the two-phonon band, extracted from curve fits to the Raman spectra. The curve fitting procedure is described in Fig. S1 of the Supplemental Material [18].

The Thalmeier-Fulde description predicts that the relative mixing of electron-phonon character associated with the vibronic modes depends on the energy difference between the coupled phonon band and the CEF level [12]. In Ce_2O_3, the appearance of a relatively narrow "phonon-like" mode at $\omega_1 \approx 177$ cm^{-1} and a broader "electron-like" mode at $\omega_2 \approx 250$ cm^{-1} is consistent with the relatively large separation between the coupled phonon band at 194 cm^{-1} and the CEF_1 level.

Unlike previously observed vibronic modes in rare-earth materials [12–16], the vibronic modes observed in Ce_2O_3 are noteworthy in that they emerge in the MD regime below T_N. Importantly, the integrated Raman scattering intensity of an excitation is proportional to the modulation of the dielectric response due to that excitation [27–30]. The

significant increase in the intensity of both the vibronic modes observed below T_N [see Fig. 3(a)] is consistent with an enhanced modulation of the dielectric susceptibility due to these modes, as expected in the MD regime in the Néel state of Ce_2O_3. In particular, the increased coupling between the CEF electronic and phononic modes below T_N is expected to result in enhanced fluctuations in the electronic levels, which is known to cause increased fluctuations of the dielectric response [31].

To extract more quantitative information from the emergent ω_1 and ω_2 modes in Ce_2O_3, we apply the Thalmeier-Fulde model for vibronic mode energies resulting from a coupling between a CEF excitation and a phonon band [12]

$$\omega_{1,2} = \frac{\omega_{\mathrm{CEF}} + \omega_{\mathrm{ph}}}{2} \mp \sqrt{\left(\frac{\omega_{\mathrm{CEF}} - \omega_{\mathrm{ph}}}{2}\right)^2 + V^2}, \quad (1)$$

where ω_{CEF} and ω_{ph} denote the energies of the CEF excitation and the phonon band, respectively, and V denotes the electron-phonon coupling strength between them. Using the measured vibronic energies, ω_1 and ω_2, and the involved CEF_1 excitation energy in Eq. (1), we can extract the temperature dependence of V and ω_{ph} (see Table II in the Supplemental Material [18]). The calculated phonon band energy ($\approx$199 cm^{-1}) is close to the experimentally observed two-phonon band centered at $\omega_{\mathrm{ph}} \approx 194$ cm^{-1}, consistent with our assumption that this band is involved in the vibronic coupling.

The resulting temperature dependence of the electron-phonon coupling strength, V, is plotted in Fig. 4(b), showing that the emergence of the vibronic modes below T_N in Ce_2O_3 results from a rapid increase in electron-phonon coupling strength through the Néel transition. Significantly, the increase in electron-phonon coupling shown in Fig. 4(b) coincides with the abrupt increase in the 416 cm^{-1} E_g symmetry stretching vibration below T_N [see Figs. 3(c) and 3(d)], which suggests a decrease in the Ce-O(II) bond length involved in this vibration. Consequently, we propose that the increasing vibronic mode coupling parameter and resultant emergence of vibronic modes in Ce_2O_3 are caused by magnetostructural changes associated with the Néel ordering, which result in an abrupt shortening of the Ce-O(II) bond below T_N.

To test the above hypothesis, we conducted magnetic field–dependent Raman measurements to study the effects of magnetic field on the vibronic and phonon modes. Figure 5(a) shows that an increasing magnetic field leads to a decrease of the vibronic mode intensities and a slight reduction of the level repulsion between the ω_1 and ω_2 modes, primarily resulting from a shift of the ω_2 mode to lower energies. Analyzing the field-dependent results using Eq. (1), the slight decrease in the energy separation between ω_1 and ω_2 vibronic modes with increasing field is consistent with a small decrease in the vibronic mode coupling with applied field, as summarized in Fig. 5(b). Consistent with this result, Fig. 6 shows that the 416 cm^{-1} E_g phonon exhibits a decrease in energy with increasing field for $T < T_N$, indicating that the associated Ce-O(II) bond lengthens slightly with increasing magnetic field in the Néel state. These results support the hypothesis that magnetostructural changes below T_N are responsible for the shortening of the Ce-O(II) bond and the emergence of vibronic modes in the MD regime of Ce_2O_3. In this regard, the emergence of vibronic modes in the MD phase of Ce_2O_3 is analogous to the emergence of electromagnons that develop via magnetostriction in the magnetoelectric phase of magnetoelectric materials [3,4].

Additionally, the decrease of the vibronic mode intensities with applied field is consistent with a reduced modulation of the dielectric response by these modes in the Néel state. Altogether, these field-dependent results

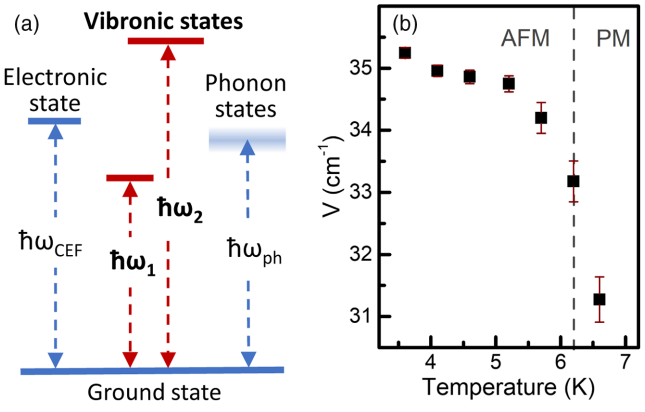

FIG. 4. (a) Schematic representation of the coupling of electronic (CEF) and vibrational states to form new bound states called "vibronic states". (b) Temperature dependence of the electron-phonon coupling constant, V [extracted from Eq. (1)]. Dashed line denotes $T = T_N$. The fitting errors in peak positions were used to estimate the error bars in V as per Eq. (1).

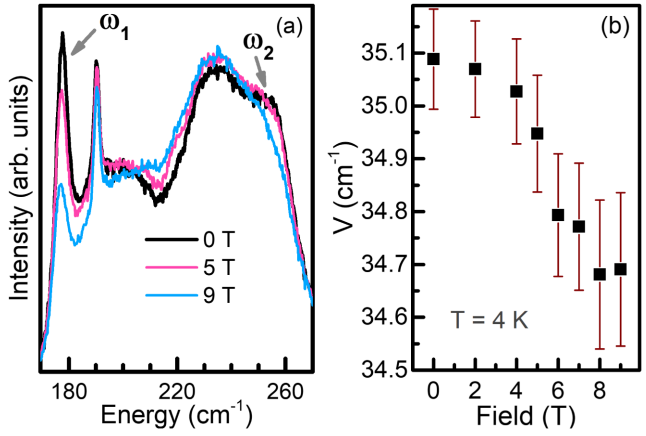

FIG. 5. (a) Raman spectrum of vibronic modes as a function of magnetic field at $T = 4$ K. (b) Summary of field dependence of electron-phonon coupling constant, V [extracted from Eq. (1)]. The fitting errors in peak positions were used to estimate the error bars in V as per Eq. (1).

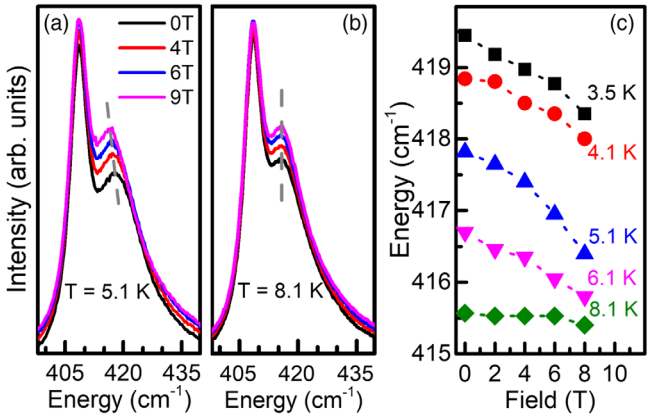

FIG. 6. Raman spectrum of stretching E_g phonon as a function of field in (a) magnetic phase, $T = 5.1$ K and (b) paramagnetic phase, $T = 8.1$ K. (c) Summary of E_g phonon energy as a function of magnetic field at various temperatures. Dotted lines are guide to the eye.

provide evidence that the field-tunable coupling between the CEF and phonon excitations is correlated with the unusual MD behavior in Ce_2O_3 below T_N, presumably because of enhanced fluctuations of the CEF levels by phonons [31].

Conclusion.—The localized f orbitals in Ce_2O_3 result in an energetic overlap between the CEF and phonon excitations, which is favorable for strong electron-phonon (vibronic) coupling. We provide evidence that magneto-structural changes below $T_N(\approx 6.2$ K) in Ce_2O_3 lead to a rapid enhancement in CEF-phonon coupling, which is manifest in the emergence of two coupled vibronic modes. Our results suggest that the strong interactions between the CEF electronic and phononic subsystems lead to increased fluctuations of the dielectric response below T_N, which we argue result from increased fluctuations of the CEF levels. The field dependence of the vibronic modes suggests that the coupling between the CEF and phonon states is reduced with increasing field. These results suggest a distinct mechanism for magnetodielectricity in rare-earth materials like Ce_2O_3, involving a field-tunable vibronic coupling. This mechanism is not expected in TM oxides because of the significantly higher CEF energies associated with d-orbital materials.

Research was supported by the National Science Foundation under Grant No. NSF DMR 1800982. T. K. was supported by NIMS internal projects Grants No. PA5160 and No. PA4020. We thank Gregory MacDougall for useful discussions.

*asethi8@illinois.edu
†slcooper@illinois.edu

[1] S.-W. Cheong and M. Mostovoy, Nat. Mater. **6**, 13 (2007).
[2] N. Mufti, A. A. Nugroho, G. R. Blake, and T. T. M. Palstra, J. Phys. Condens. Matter **22**, 075902 (2010).
[3] R. Valdés Aguilar, M. Mostovoy, A. B. Sushkov, C. L. Zhang, Y. J. Choi, S.-W. Cheong, and H. D. Drew, Phys. Rev. Lett. **102**, 047203 (2009).
[4] A. B. Sushkov, R. V. Aguilar, S. Park, S.-W. Cheong, and H. D. Drew, Phys. Rev. Lett. **98**, 027202 (2007).
[5] A. Pimenov, A. A. Mukhin, V. Y. Ivanov, V. D. Travkin, A. M. Balbashov, and A. Loidl, Nat. Phys. **2**, 97 (2006).
[6] S. Dong, J.-M. Liu, S.-W. Cheong, and Z. Ren, Adv. Phys. **64**, 519 (2015).
[7] N. Ortega, A. Kumar, J. F. Scott, and R. S. Katiyar, J. Phys. Condens. Matter **27**, 504002 (2015).
[8] D. M. Juraschek, M. Fechner, A. V. Balatsky, and N. A. Spaldin, Phys. Rev. Mater. **1**, 014401 (2017).
[9] H. Katsura, A. V. Balatsky, and N. Nagaosa, Phys. Rev. Lett. **98**, 027203 (2007).
[10] T. Kolodiazhnyi, H. Sakurai, M. Avdeev, T. Charoonsuk, K. V. Lamonova, Y. G. Pashkevich, and B. J. Kennedy, Phys. Rev. B **98**, 054423 (2018).
[11] J. B. Gruber, B. H. Justice, J. Edgar F. Westrum, and B. Zandi, J. Chem. Thermodyn. **34**, 457 (2002).
[12] P. Thalmeier and P. Fulde, Phys. Rev. Lett. **49**, 1588 (1982).
[13] M. Loewenhaupt and U. Witte, J. Phys. Condens. Matter **15**, S519 (2003).
[14] J. Gaudet, A. M. Hallas, C. R. C. Buhariwalla, G. Sala, M. B. Stone, M. Tachibana, K. Baroudi, R. J. Cava, and B. D. Gaulin, Phys. Rev. B **98**, 014419 (2018).
[15] D. T. Adroja, A. del Moral, C. de la Fuente, A. Fraile, E. A. Goremychkin, J. W. Taylor, A. D. Hillier, and F. Fernandez-Alonso, Phys. Rev. Lett. **108**, 216402 (2012).
[16] E. T. Heyen, R. Wegerer, E. Schönherr, and M. Cardona, Phys. Rev. B **44**, 10195 (1991).
[17] K. N. Boldyrev *et al.*, Phys. Rev. B **90**, 121101(R) (2014).
[18] See Supplemental Material at http://link.aps.org/supplemental/10.1103/PhysRevLett.122.177601 for details of (i) quantifying laser heating and (ii) curve fittings to the Raman spectra.
[19] D. Avisar and T. Livneh, Vib. Spectrosc. **86**, 14 (2016).
[20] J. Gouteron, D. Michel, A. Lejus, and J. Zarembowitch, J. Solid State Chem. **38**, 288 (1981).
[21] J. Zarembowitch, J. Gouteron, and A. M. Lejus, Phys. Status Solidi (b) **94**, 249 (1979).
[22] J. Pierre, R. Galera, and J. Bouillot, J. Magn. Magn. Mater. **42**, 139 (1984).
[23] R. Osborn, M. Loewenhaupt, B. Rainford, and W. Stirling, in *Anomalous Rare Earths and Actinides*, edited by J. Boucherle, J. Flouquet, C. Lacroix, and J. Rossat-Mignod (Elsevier, New York, 1987), pp. 70–72.
[24] R. Schedler, M. Rotter, U. Witte, M. Loewenhaupt, and W. Schmidt, Acta Phys. Pol. B **34**, 1313 (2003).
[25] A. D. Hillier, D. T. Adroja, P. Manuel, V. K. Anand, J. W. Taylor, K. A. McEwen, B. D. Rainford, and M. M. Koza, Phys. Rev. B **85**, 134405 (2012).
[26] M. Smidman, D. T. Adroja, A. D. Hillier, L. C. Chapon, J. W. Taylor, V. K. Anand, R. P. Singh, M. R. Lees, E. A. Goremychkin, M. M. Koza, V. V. Krishnamurthy,

D. M. Paul, and G. Balakrishnan, Phys. Rev. B **88**, 134416 (2013).
[27] W. Hayes and R. Loudon, *Scattering of Light by Crystals* (Dover Publications, Mineola, 1978).
[28] S. Lushnikov, S. Gvasaliya, and R. S. Katiyar, Phys. Rev. B **70**, 172101 (2004).
[29] A. Kumar, J. F. Scott, and R. S. Katiyar, Appl. Phys. Lett. **99**, 062504 (2011).
[30] A. Sethi *et al.*, Phys. Rev. B **95**, 174413(R) (2014).
[31] S. H. Wemple and M. DiDomenico, in *Light Scattering Spectra of Solids*, edited by G. B. Wright (Springer, Berlin, Heidelberg, 1969), pp. 65–74.